

Case Report

Spatial Monitoring of Urban Expansion Using Satellite Remote Sensing Images: A Case Study of Amman City, Jordan

Hussam Al-Bilbisi

Geography Department, The University of Jordan, Amman 11942, Jordan; hbilbisi@ju.edu.jo

Received: 29 January 2019; Accepted: 12 April 2019; Published: 15 April 2019



Abstract: Amman, the capital city of Jordan, faces urbanization challenges and lacks reliable data for urban planning. This study is aimed at assessing, monitoring, and mapping urban land cover using multitemporal Landsat satellite images. Four different land use/cover maps were produced; periods of over ten years between 1987 and 2017 (i.e., in 1987, 1997, 2007, and 2017) were used to evaluate and analyze urban expansion visually and quantitatively. Supervised classification technique followed by the post classification comparison change detection approach was used to analyze images. Over the past three decades, the urban area has increased rapidly in Amman. It increased by 90.78 km², from 149.08 km² in 1987 to 237.86 km² in 2017, with an average annual rate of increase of 2.03%. Urban area increases were significantly higher in the first 10 years of the study period (i.e., from 1987 to 1997), during which the average annual rate of increase reached 3.33%, while it was 2.04% for the last two decades of the study period (i.e., from 1997 to 2017). Urban growth in Amman generally occurred along transport routes away from the core of Amman, and as a result, this growth led to the expansion of urban areas into other types of land use/cover classes, particularly vegetation areas. The spatial analysis of urban expansion and trends of urban growth in Amman could provide the required input data for the urban modeling of the city.

Keywords: Amman; urban expansion; Landsat; remote sensing; Jordan

1. Introduction

Urban expansion is defined as a spatiotemporal arrangement process involving various urban growth types [1]. Moreover, urban expansion results from the combined effects of anthropogenic and natural factors [2]. Anthropogenic factors mainly include population and economy growth, as well as urban traffic development, while natural factors contributing to spatial heterogeneity mainly include topography and soil characteristics. Both factors may significantly change landscape structures, causing changes in different types of land use/cover in the urban expansion and transformation [2]. In developing countries, urban growth and expansion generate many problems and challenges socially, environmentally, and economically by altering land use/cover patterns, land values, and the intensity of site use [3]. In many cities, urban growth, on the one hand, is an indicator of social, economic, and political growth, whereas, on the other hand, it has negative impacts on agricultural land and the greenery of the city [4]. Urban expansion also causes landscape transformations and degradation through fragmental and ecological changes [5]. Several studies [6–8] addressed that landscape transformation resulting from the urban expansions has induced serious environmental issues threatening sustainable development. Landscape transformations under the influence of urbanization are multidirectional and differentiated in time and space [9]. The dynamic process of urban expansion depends on topography and land use of the influenced area, as well as on the demography and economy of a city [10]. Urban expansion causes changes of natural landscape which

is mainly composed of vegetation, soil, and rocks to manmade landscape which is mainly composed of asphalt, concrete, and metals [9,11,12]. One of the major problems of urban expansion is landscape transformations into developed land use [13]. Consequently, landscape transformations and urban expansion increase pressure on the surrounding land and other resources and cause changes in quality of life, either positively or negatively.

At present, remote sensing has been recognized as a valuable technique for viewing, monitoring, analyzing, characterizing, and mapping urban growth and expansion. It has therefore been widely used in detecting and monitoring urban changes on various scales with useful results [1,4,14–17]. Remote sensing is an important source of information for urban expansion analysis based on its high spatial and temporal accuracy and consistency [18]. Moreover, remote sensing data are very useful because of their synoptic view, repetitive coverage, and real-time data acquisition. Digital data, in the form of satellite images, enable the accurate differentiation of land use/cover categories and help to maintain the spatial data infrastructure, which is essential for monitoring urban expansion [19]. A database needs to be created in order to show urban area changes in a particular area at regular intervals as far back in time as possible. Obviously, satellite data, remote sensing, and Geographic Information Systems (GIS) are the most relevant technologies for meeting these needs in the most effective manner [15].

Amman accommodates many activities and multiple functionalities, and any changes in such patterns are obvious. In the last 30 years, the spatial organization of Amman and its original structure has changed dramatically, and thus, the city is segmented in different regions, each involving a particular activity. Amman's population has grown rapidly over the past three decades. The population increased by more than 95% between 1987 and 2017 [20]. Amman is undergoing both a very high rate of urbanization and human-induced changes in land use/cover. Urban land use is the major category of land use that is primarily influenced by the activities of human beings [19]. Using Landsat images, the objective of this study is to assess, monitor, and map urban expansion over the past three decades (from 1987 to 2017) in Amman in order to provide the required input data for urban modeling.

2. The Study Area

The study area is the capital city of Jordan (Amman city), which is located in the central part of Jordan; it divides into 22 districts with a total area of 758.85 km². It lies between the latitudes 31°45'00" and 32°05'00" N and longitudes 35°44'00" and 36°14'00" E. Figure 1 shows the location of the study area, the districts of Amman, and the population density (in 2017); some districts have a high population density while others have low density. Areas of high population density tend to be located in the core of the city. Amman is an important political, economic, and cultural city. During the last four decades, Amman's population increased by more than three times. According to the official results of the Housing & Population Census, Amman's population was about 778,000 inhabitants in 1979, representing 30% of the total of Jordan's population. By 1987, the total population was estimated to be 1.013 million inhabitants. It was estimated to be 1.465 million inhabitants in 1997. In 2007 Amman's population was estimated to be 2.170 million inhabitants. The results of the last census, which was held in 2015, revealed that Amman's population exceeds 3.85 million inhabitants, representing 39.7% of the total population of Jordan (about 9.56 million inhabitants); the estimated population of Amman in 2017 was approximately 4.090 million inhabitants [20]. Amman's population growth over the last several decades was influenced by many factors, including the internal migration to Amman, where jobs are available, as well as the wars and crises that have affected the region, such as the First Gulf War of 1991, the invasion of Iraq in 2003, and the Civil War in Syria in 2011, all of which led to dramatic population fluxes into Jordan. Hundreds of thousands of Jordanian people returned to Jordan in 1991 and 2003 from Gulf countries, and more than one million Syrian refugees entered Jordan. Most of those people reside in urban areas, especially in Amman city, given the availability of services and job opportunities, and as a result, the concentration of people in Amman's urban areas, which include residential units, educational facilities, and industrial plants, has increased.

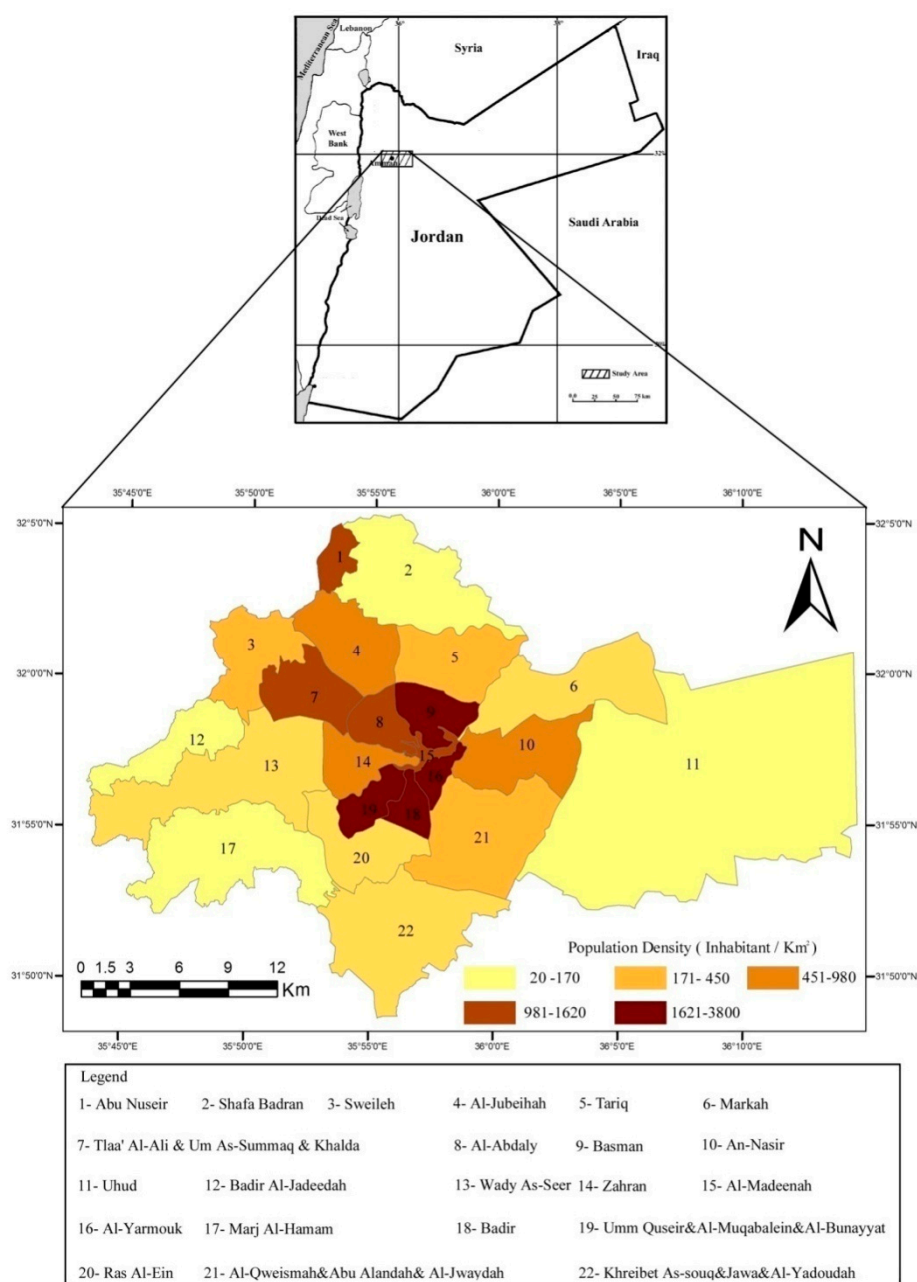


Figure 1. Location of the study area. The inset shows the districts of Amman and the population density (in 2017).

Amman is located on an undulating plateau that comprises the northwest of Jordan. The topography of the city consists of a series of steep hills and deep and sometimes narrow valleys. Limestone rocks interbedded with chert, marl, and chalk beds are the dominant rocks in the study area [21,22]. The soil in the studied area is derived from limestone, and the soil depth decreases as the inclination becomes steeper than 4%. The most important characteristics of this soil are high proportions of silt and calcium carbonates [23]. Vegetation in the study area includes irrigated vegetables and rain-fed crops of wheat, barley, olives, and fruit trees. Deciduous and evergreen oaks and pine forests are scattered in the western parts of the study area. The eastern parts are used as open rangelands [24].

A typical Mediterranean climate dominates the study area [24]. Summer, which extends from late May to the end of September, is hot and dry. The mean annual temperature usually ranges between 28 °C and 32 °C, with low humidity and frequent breezes. Winter, which extends from November

to April, is wet and cold. The mean annual temperature during daytime in winter usually ranges between 12 °C and 22 °C. In December and January, nighttime temperature reaches 0 °C or below, and snow occurs on occasion. The relative humidity ranges between 50% and 60% with an average annual rainfall of more than 300mm, with the highest amount of rainfall typically occurring in January and February. In recent years, however, these patterns have been less reliable, with the highest amount of rainfall occurring in April and May [25].

3. Materials and Methods

3.1. Geometric Rectification and Radiometric Calibration

A timeseries of Landsat Thematic Mapper (TM), Landsat Enhanced Thematic Mapper Plus (ETM+), and Landsat 8 Operational Land Imager (OLI) images were used for monitoring urban expansion in and deriving land use/cover maps of the study area. The dataset included full scenes for the years 1987, 1997, 2007, and 2017. The selected datasets were cloud-free images acquired in September. The dataset was mainly downloaded from the archive of the Global Land Cover Facility (GLCF) (<http://glcf.umiacs.umd.edu/index.shtml>) and the official website of Landsat 8 (<http://earthexplorer.usgs.gov>) at no cost. The images included the visible, near-infrared (NIR), and mid-infrared (MIR) bands with 30 m spatial resolution for the TM and ETM+ images. The equivalent bands were selected from the OLI image of 2017.

Various image processing techniques were applied to prepare the images for visual interpretation of urban expansion and land use/cover mapping. These included geometric correction, radiometric calibration, and clipping of the images to the borders of the study area. The digital images were geometrically and radiometrically calibrated to each other to facilitate their comparison. Geometric rectification is critical for producing spatially correct maps of urban expansion and land use/cover changes over time. The 2017 Landsat (OLI) image had already been rectified and georeferenced to the Universal Transverse Mercator (UTM) map projection (Zone 36), and WGS84 ellipsoid. Then, this image was employed as the reference scene to which the other scenes of 1987, 1997, and 2007 were registered. Using image-to-image registration, a first-degree polynomial equation was used in image transformation. The resultant Root-Mean-Square Error (RMSE) was less than 15m, indicating an excellent registration. The nearest-neighbor resampling method was used to avoid altering the original pixel values of the image data [26]. Histogram matching was used to improve the visual appearance and brightness of the output image [27].

3.2. Image Processing and Classification

TM and ETM+ bands (2, 3, and 4) and bands (2, 4, and 7) and their equivalent OLI bands (3, 4, and 5) and bands (3, 5, and 7) color combinations were generated from each image of TM 1987, TM 1996, ETM+ 2007, and OLI 2017 for visual interpretation and analysis purposes. The selection of color combinations of the TM and ETM+ bands 2, 4, and 7 and OLI bands 3, 5, and 7 were generated in order to use the information of the three main spectral regions of Landsat imagery (i.e., visible, near-infrared, and mid-infrared regions).

To map the urban expansion and changes that had occurred during the study period, six spectral bands of all digital data (with the thermal bands being excluded) were individually used as input for supervised classification purposes. The maximum likelihood algorithm provided by PCI software was used for land use/cover mapping from multitemporal Landsat images.

A modified version of the Sato–Tateishi Land Cover Guideline (ST-LCG) [28] scheme was adopted and used as a classification scheme design for this study. In total, four land use/cover classes were included in this study: (1) urban area, (2) vegetation, (3) exposed rocks, and (4) exposed soils. Detailed definitions of these four categories of land use/cover are summarized in Table 1.

Table 1. Use and land cover classes and definitions used in this study.

No	Class	Definitions
1	Urban Area	Construction materials (e.g., asphalt, concrete, etc.), typically commercial and industrial buildings, residential developments including mostly single/multiple houses, and transportation facilities (e.g., airports, parking lots, highways, local roads).
2	Vegetation	Field crops, trees (mainly olives and fruit trees), deciduous and evergreen oaks and coniferous trees including both protected and open forests, and open shrub and herbaceous rangelands.
3	Exposed Rocks	Consolidated lands (bare rock areas, gravels, stones, and boulders).
4	Exposed Soils	Unconsolidated lands (bare soil areas).

Given that the spectral confusion of the land use/cover classes which have similar spectral responses is the major cause of classification inaccuracy of spectrally based classification methods [29–31], visual interpretation and on-screen digitizing were used to solve the spectral confusion of the adopted land use/cover classes. With the use of this method, two major types of spectral confusion can be identified in the current study: (1) urban area/exposed rocks classes and (2) vegetation/exposed soils classes. These spectrally confused classes were further differentiated and recorded into their correct land use/cover classes.

4. Results and Discussion

Figures 2–4 show the color composites generated (bands 7, 4, and 2) from the filtered TM images of 1987 and 1997 and the ETM+ image of 2007, respectively, while Figure 5 shows the color composite generated (bands 7, 5, and 3) from the filtered OLI image of 2017. The urban area is depicted as pink color, while vegetation is green, because the near-infrared band, in which vegetation has a high spectral response, was exposed through the green filter. Color products using the combinations of bands 4, 3, and 2 for the TM and ETM+ images and bands 5, 4, and 3 for the OLI image were also generated for interpretation and analysis purposes. The urban area in this combination is shown as a cyan color, while vegetation is red.

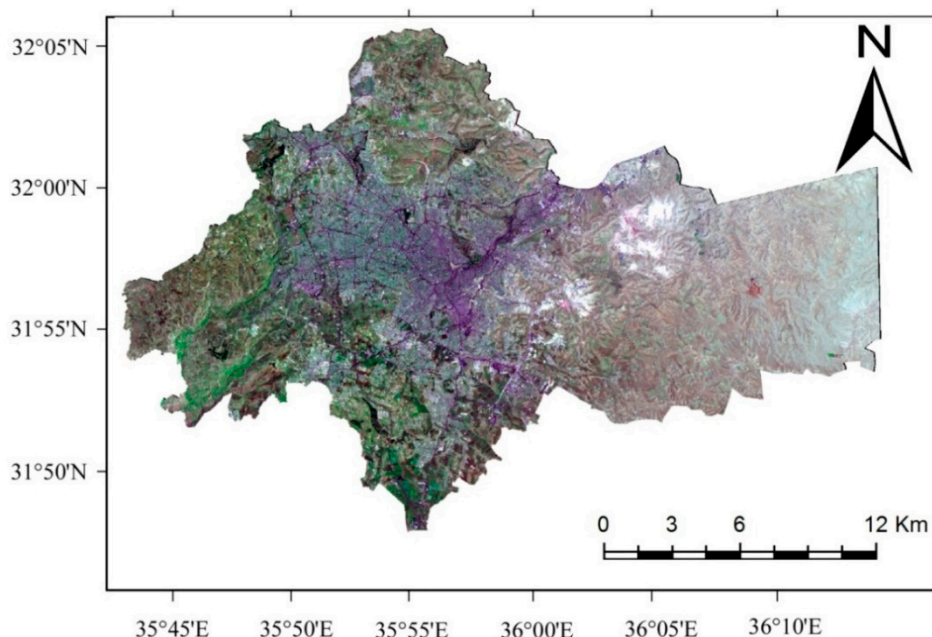


Figure 2. Color composite image bands 7, 4, and 2 of the TM image of 1987, exposed through the red, green, and blue filters, respectively.

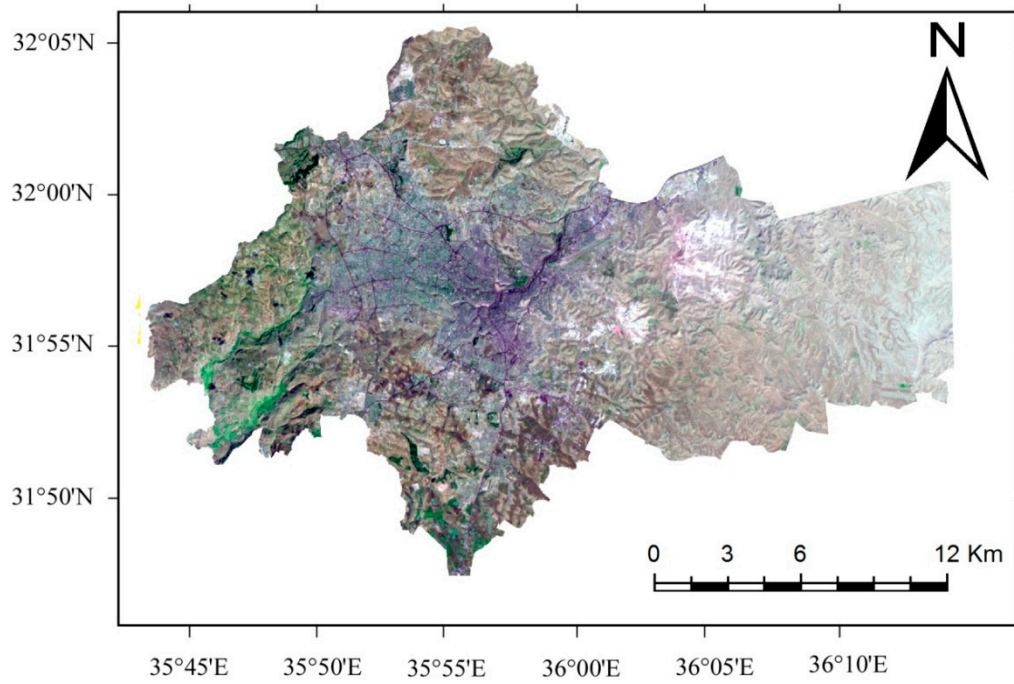


Figure 3. Color composite bands 7, 4, and 2 of the TM image of 1997, exposed through the red, green, and blue filters, respectively.

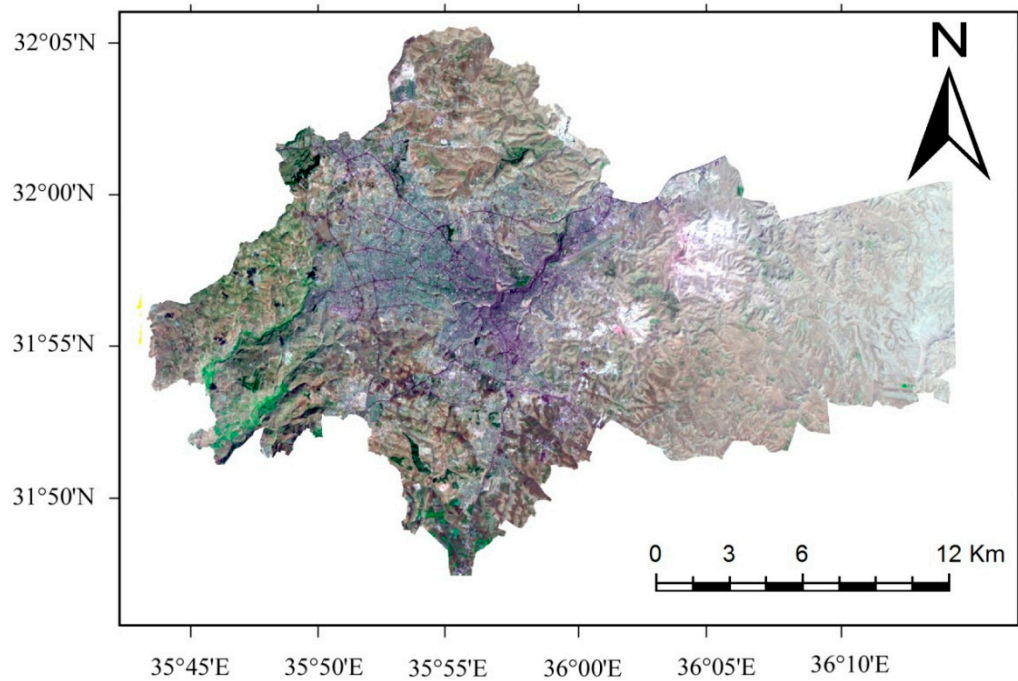


Figure 4. Color composite bands 7, 4, and 2 of the ETM+ image of 2007, exposed through the red, green, and blue filters, respectively.

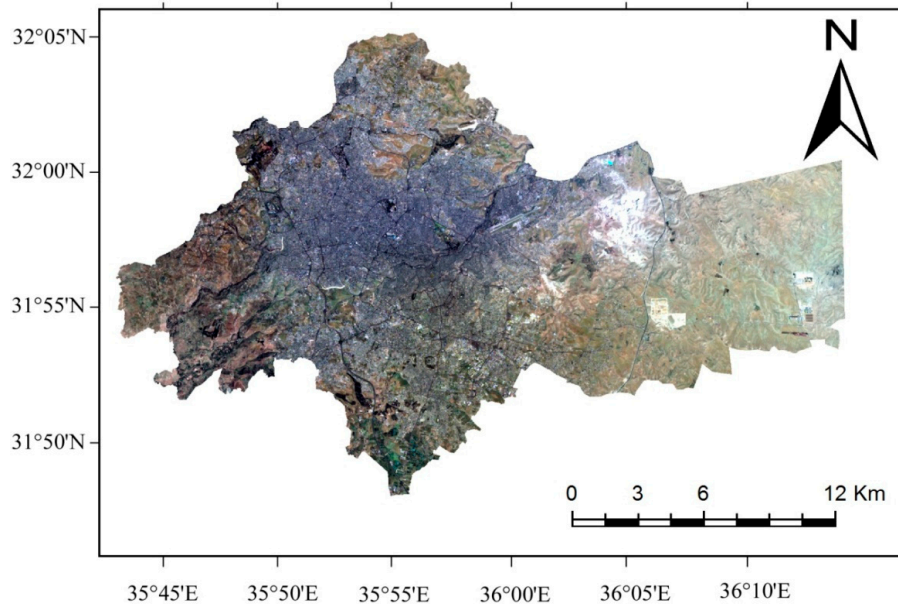


Figure 5. Color composite bands 7, 4, and 2 of the Landsat 8 (OLI) image of 2017, exposed through the red, green, and blue filters, respectively.

4.1. Urban Expansion Monitoring and Change Detection

Figures 6–9 show the results of the supervised classification of TM 1987, TM 1997, ETM+ 2007, and OLI 2017, respectively. Using PCI software, a random sampling method was employed to obtain overall accuracy. A total of 120 pixels were selected. These were checked via an in situ check and through high-resolution images provided by Google Earth. The results indicated an overall classification accuracy of about 86.4%, 85.7%, 88.6%, and 90.2% for the 1987, 1997, 2007, and 2017 images, respectively. The overall accuracy results revealed that all of the classified maps' accuracies were more than 85%, which indicate that the image processing approach adopted in this study was effective in producing compatible land use/cover data over time.

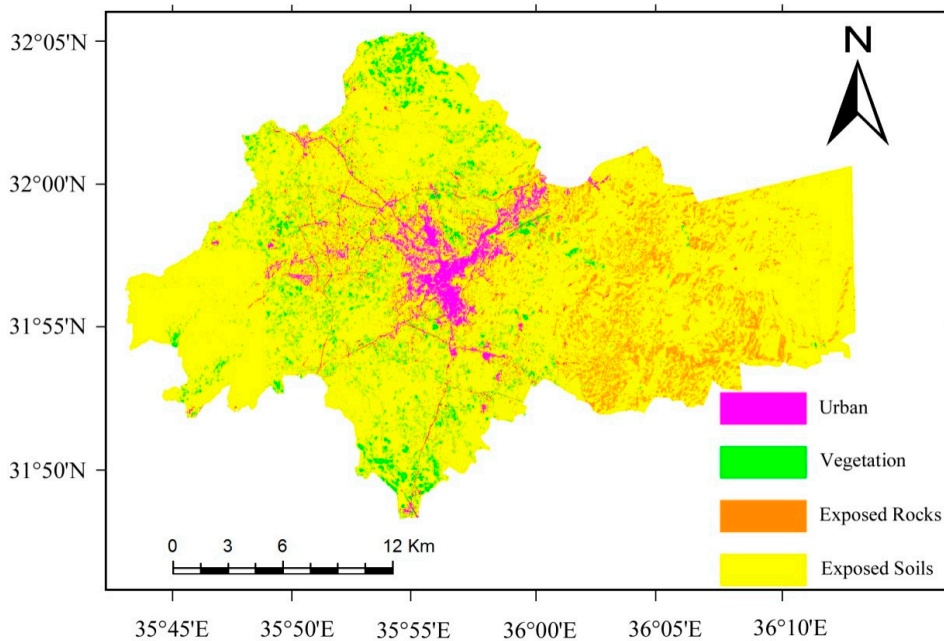


Figure 6. Land use/cover classification map of Amman based on the analysis of Landsat TM 1987.

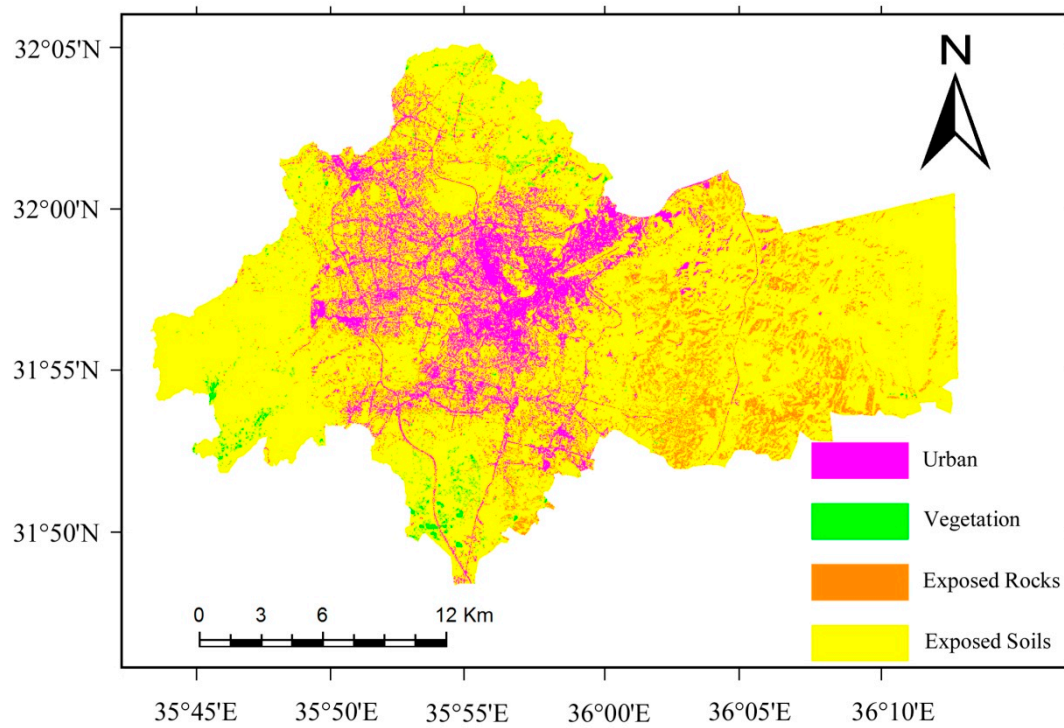


Figure 7. Land use/cover classification map of Amman based on the analysis of Landsat TM 1997.

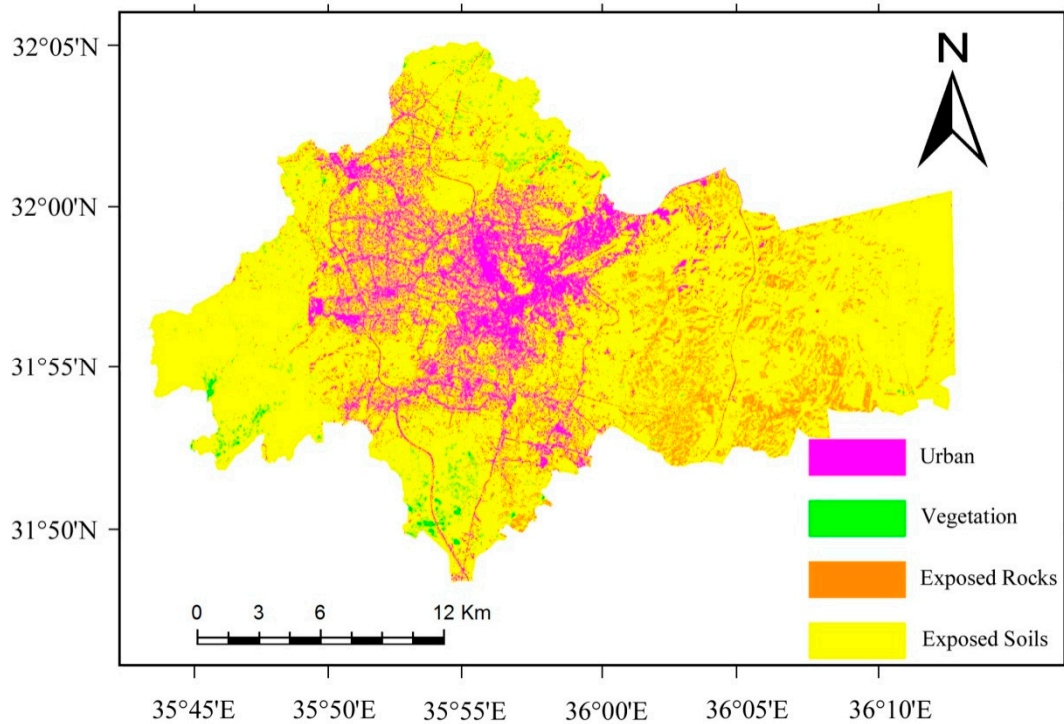


Figure 8. Land use/cover classification map of Amman based on the analysis of Landsat ETM+ 2007.

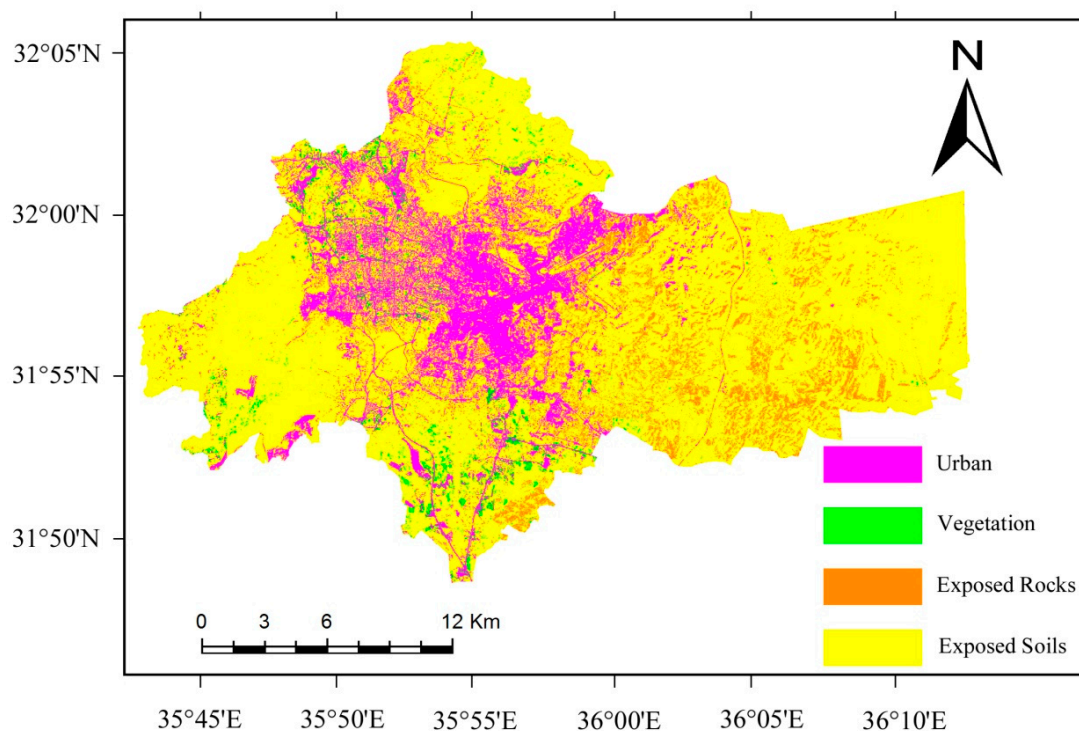


Figure 9. Land use/cover classification map of Amman based on the analysis of Landsat OLI 2017.

There are four major land use/cover classes of interest in Amman: urban area, vegetation, exposed rocks, and exposed soils. The spatial distribution of these classes was extracted from each of the land use/cover maps of 1987, 1997, 2007, and 2017, and the results are shown in Table 2.

Table 2. Land use/cover change for the studied area as extracted from the digital images.

Class Name	1987Area (km ²)/(%)		1997Area (km ²)/(%)		2007Area (km ²)/(%)		2017Area (km ²)/(%)		% of Increase or Decrease Since 1987
Urban Area	147.08	19.39	195.98	25.84	214.94	28.34	237.86	31.36	+61.73%
Vegetation	35.22	4.64	28.25	3.72	23.71	3.13	16.40	2.16	−53.54%
Exposed Rocks	54.32	7.16	45.85	6.04	37.41	4.93	30.34	4.00	−44.13%
Exposed Soils	521.94	68.81	488.48	64.40	482.50	63.60	473.96	62.48	−9.23%

The post classification comparison change detection approach was also employed here [32]. This method involves comparing multitemporal independently produced classified land use/cover maps from multitemporal images. It was found to be an accurate procedure for land use/cover change detection, provided that the multitemporal land use/cover maps had been accurately produced, as they were in this study.

In Figures 6–9, the spatial expansion of the urban area class is clearly visible. The urban area was small and was mainly located in the inner parts of Amman until 1987. The spread of the urban area class is clearly revealed in the 2017 map. The comparison of class statistics shows that there has been marked urban expansion in a span of 30 years. However, the results show a substantial increase in only one land use/cover class, namely the urban area class. Over the past three decades, urban area has increased rapidly in Amman (Table 2). It increased by 90.78 km², from 149.08 km² in 1987 to 237.86 km² in 2017. This is an average annual rate of increase of 2.06%. Therefore, the 2017 urban area was 1.6 times the size of the urban area in 1987. There were different stages in the urbanization process of Amman during the study period (1987–2017) (Figure 10). In the first decade of the study

period (1987–1997), the urban area expansion was significantly high. During this period and as a result of the first Gulf War in 1991, more than 300,000 persons returned to Jordan from Kuwait and other Gulf countries, and most of them settled in urban areas, particularly in Amman. Many of those people either built their private houses on their own lands or bought (or rented) houses; consequently, many buildings and houses were constructed. In quantitative terms, the urban area class has increased from 147.08 km² in 1987 to 195.98 km² in 1997 (Table 2), thus representing an increase of more than 6% of the total area. Figures 6 and 7 show the burgeoning spatial urban expansion of the city and its rapid growth occurred in all directions between 1987 and 1997.

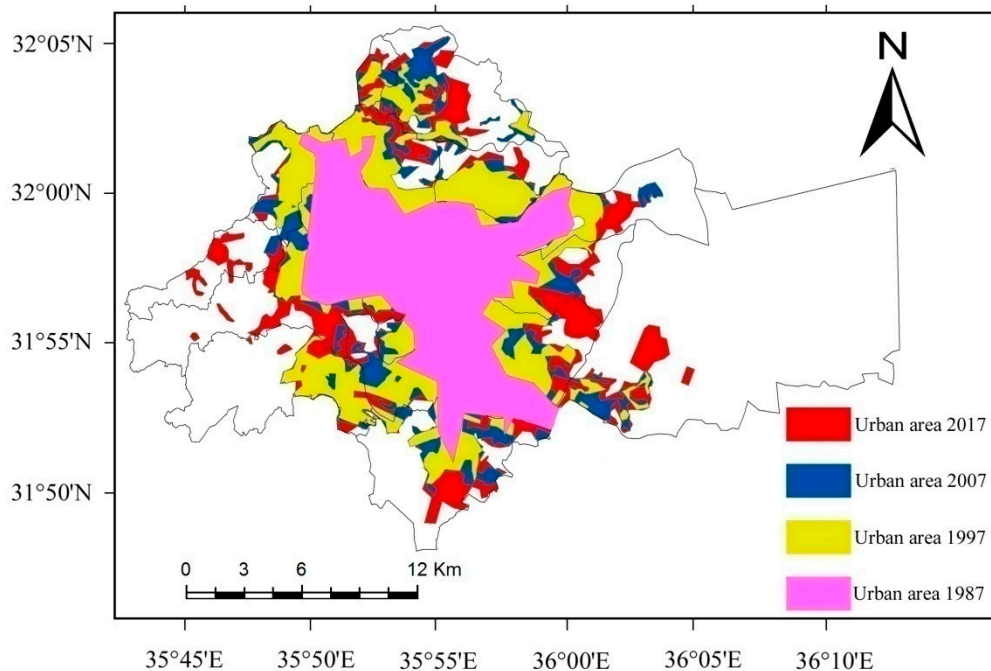


Figure 10. The spatial development of Amman's urban area between 1987 and 2017.

During the second decade of the study period (1997–2007), the invasion of Iraq in 2003 led to another population flux into Jordan, and as a result, the concentration of people in urban areas increased. The urban area class increased by 18.96 km², from 195.98 km² in 1997 to 214.94 in 2007 (Figures 7 and 8).

Although Jordan received hundreds of thousands of Syrian refugees between 2011 and 2017, during the last decade of the study period (2007–2017), urban expansion accelerated at a stabilized development rate. Urban expansion occurred at approximately the rate of the previous period (1997–2007), which indicated a steady growth rate after 1997; this was because most of Syrian refugees were settled inside camps near to the Syrian border. In quantitative terms, the urban area class increased by 22.92 km², from 214.94 km² in 2007 to 237.86 km² in 2017 (Table 2), thus representing an increase of about 3% of the total area. Urban expansion and changes of land use/cover in the northwestern, southwestern, and southeastern parts of Amman, where many housing settlements were established in these areas between 1997 and 2017 (Figures 8 and 9), were particularly noteworthy. Figure 10 shows the spatial development of the urban expansion of Amman between 1987 and 2017.

Another significant change is the continuing decline in the vegetation class in the studied area (Figure 11). In 1987, the vegetation class occupied 35.22 km², which decreased to 16.40 km² by 2017, signifying a decrease of 18.82 km²; this represents a decrease of 53.54% (Table 2). Similarly, the exposed rocks class and exposed soils class declined between 1987 and 2017 by about 24 km² and about 48 km², respectively (Figure 11).

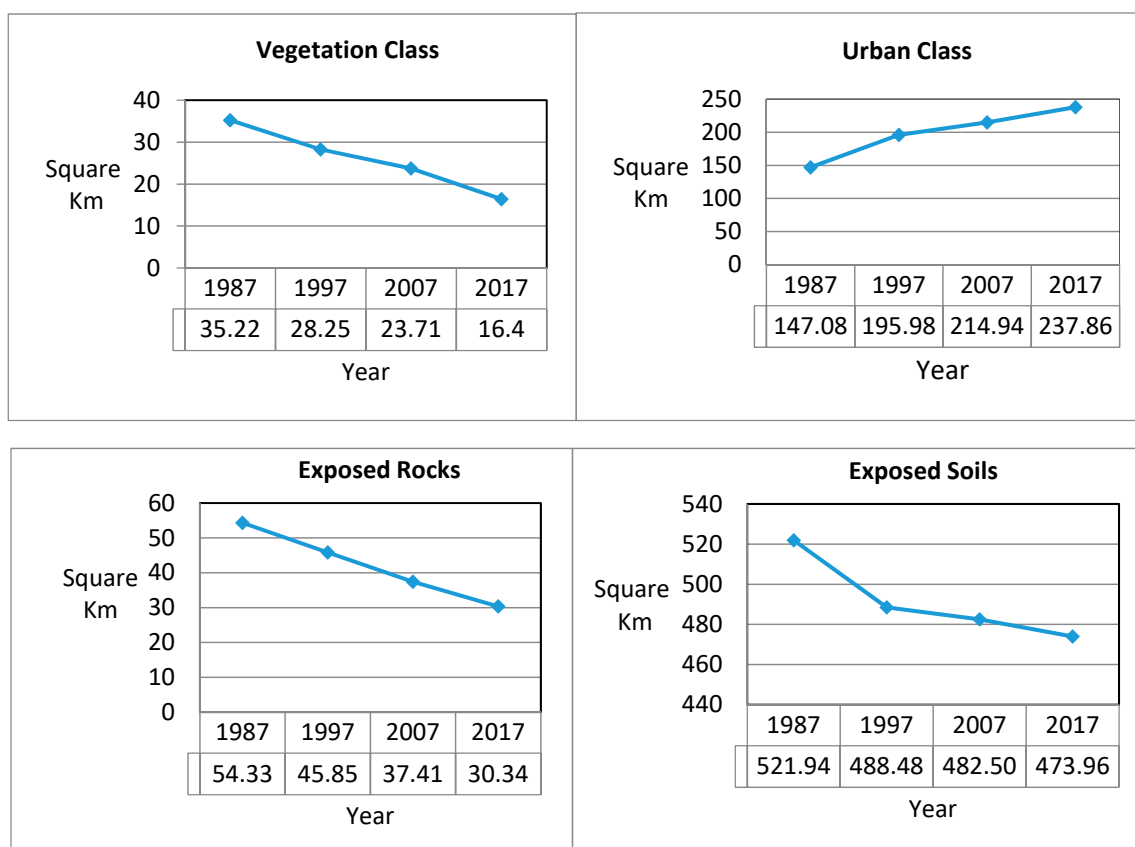


Figure 11. Changes in the urban area, vegetation, exposed rock, and exposed soil classes between 1987 and 2017.

4.2. Urban Growth Analysis (1987–2017)

Table 3 shows the annual urban growth percentage rate (*K*). *K* is a key index for evaluating urban growth, and is defined as follows [33]:

$$K = \left(\frac{Ub - Ua}{Ua} \right) \times \frac{1}{T} \times 100\% \tag{1}$$

where *K* is the annual urban growth percentage rate, *Ua* and *Ub* represent the urban area at the beginning and end of the monitoring period, respectively, and *T* is the period of time from time *a* to *b*.

Table 3. Amman’s annual urban growth percentage rate (1987–2017).

Year	Urban Area (km ²)	Annual Growth(%)
1987	147.08	—
1997	195.98	3.33
2007	214.94	0.97
2017	237.86	1.07

In this study, the results show that urban growth in Amman occurred mainly in two stages during the study period (1987–2017). The first stage was from 1987 to 1997, and the second one was from 1997 to 2007 and 2007 to 2017. During the first stage, urban area expanded by 48.9 km² (or 4.89 km² yearly). Urban area increased from 147.08 km² (or 19.39%) of the total area to 195.98 km² (or 25.84%) between 1987 and 1997; the annual urban growth rate reached 3.33%. During this stage, horizontal urban expansion was dominant, and urban growth in Amman occurred along transport routes away

from the core of Amman. Concentric urban theory explains the urban growth during the first stage (1987–1997).

In the second stage which extended from 1997–2007 and 2007–2017, urban growth continued at almost stabilized expansion rates. The urban area expanded by 18.96 km² and 22.92 km² (or 1.896 km² and 2.292 km² yearly) during the two time periods, respectively. In this stage, concentric and multiple nuclei urban theories explain the urban growth of Amman. Infrastructure projects, such as roads, water supply, and electricity, led to the expansion of urban centers resulting from improved accessibility and service delivery. Vertical urban expansion was dominant in Amman between 1997 and 2017. The annual growth rates were 0.97% (1997–2007) and 1.07% (2007–2017), indicating that Amman's urban growth has almost been steady over the last two decades.

5. Conclusions

For mapping surface changes of Amman and monitoring urban expansion over the last three decades, digital land use/cover maps, dealing with four land use/cover classes, were produced using the supervised classification scheme of Landsat images for the years 1987, 1997, 2007, and 2017. The results show that the urban area increased from 147.08 km² in 1987 to 237.86 km² in 2017. The urban area has increased by almost 61.73% over 30 years. During the same 30-year period, urban growth experienced two different urban expansion and growth stages as follows: a high-rate stage during 1987–1997 and a steady-rate stage during 1997–2007 and 2007–2017. Concentric urban growth was the main type of urban growth from 1987 to 1997; this type of growth mainly occurred along transport routes away from the core of Amman, where a number of universities and schools, as well as lots of buildings and offices, were established during this period. Horizontal urban expansion was the dominant phenomenon during this period. Concentric and multiple nuclei urban growth were the main types of urban growth models in Amman from 1997 to 2017, where infrastructure projects led to the expansion of urban centers. Moreover, vertical urban expansion was the dominant phenomenon during the last two decades of the study period. The results of a recent study [17] investigating urban expansion in Isfahan, Iran, using remotely sensed data, including aerial photos and satellite images acquired from Landsat MSS, TM, and ETM+, showed that rapid urban growth mainly occurred along the main roads and on agricultural lands. The present study shows results that are similar to those of the Isfahan city study.

The results of this study on urban expansion provide scientific criteria to support decision making and would allow an urban planner to understand and evaluate urban growth to develop a strategy for sustainable usage of the urban land system. It is important to point out that to keep the urban growth rate low in Amman, vertical construction is strongly recommended.

In order to address urban expansion challenges without compromising the city environment, future work should explore the influences of urban expansion on landscape transformation and the land use/cover changes that took place in Amman.

Funding: This research received no external funds.

Conflicts of Interest: The author declares no conflict of interest.

References

1. Wu, Y.; Li, S.; Yu, S. Monitoring urban expansion and its effects on land use and land cover changes in Guangzhou city, China. *Environ. Monit. Assess.* **2016**, *188*, 54. [[CrossRef](#)]
2. Lambin, E.F.; Turner, B.L.; Geist, H.J.; Agbola, S.B.; Angelsen, A.; Bruce, J.W.; Coomes, O.T.; Dirzo, R.; Fischer, G.; Folke, C.; et al. The cause of land cover change moving beyond the myths. *Glob. Environ. Chang.* **2001**, *11*, 261–269. [[CrossRef](#)]
3. Katyambo, M.M.; Ngigi, M.M. Spatial monitoring of urban growth using GIS and remote sensing: A case study of Nairobi metropolitan area, Kenya. *Am. J. Geogr. Inf. Syst.* **2017**, *6*, 64–82.
4. Karanam, H.K.; Neela, V.B. Study of normalized difference built-up (NDBI) index in automatically mapping urban areas from Landsat TN imagery. *Int. J. Eng. Sci. Math.* **2017**, *8*, 239–248.

5. Dewan, A.M.; Kabir, M.H.; Nahar, K.; Rahman, M.Z. Urbanization and environmental degradation in Dhaka metropolitan area of Bangladesh. *Int. J. Environ. Sustain. Dev.* **2012**, *11*, 118–147. [[CrossRef](#)]
6. Li, X.; Yeh, A.G.O. Analyzing spatial restructuring of land use patterns in a fast growing region using remote sensing and GIS. *Landsc. Urban Plane J.* **2004**, *64*, 67–76. [[CrossRef](#)]
7. Chen, S.; Zeng, S.; Xie, C. Remote sensing and GIS for urban growth analysis in China. *Photogramm. Eng. Remote Sens.* **2000**, *66*, 593–598.
8. Liu, H.; Weng, Q. Scaling-up effect on the relationship between landscape pattern and land surface temperature. *Photogramm. Eng. Remote Sens. J.* **2009**, *75*, 291–304. [[CrossRef](#)]
9. Adersson, E. Urban landscape and sustainable cities. *Ecol. Soc.* **2006**, *11*, 34. [[CrossRef](#)]
10. Zhou, N.; Zhao, S. Urbanization process and induced environmental geological hazards in China. *Nat. Hazard* **2013**, *67*, 797–810. [[CrossRef](#)]
11. Bhatta, B. Analysis of urban growth pattern using remote sensing and GIS: A case study of Kolkata, India. *Int. J. Remote Sens.* **2009**, *30*, 4733–4746. [[CrossRef](#)]
12. Zhou, D.; Shi, P.; Wu, X.; Ma, J.; Yu, J. Effects of urbanization expansion on landscape pattern and region ecological risk in Chinese coastal city: A case study of Yantai city. *Sci. World J.* **2014**, *2014*, 821781. [[CrossRef](#)]
13. Batisani, N.; Yarnal, B. Urban expansion in Centre County, Pennsylvania: Spatial dynamics and landscape transformations. *Appl. Geogr.* **2009**, *29*, 235–249. [[CrossRef](#)]
14. Pirnazar, M.; Ali-Askari, K.; Eslamian, S.; Singh, V.; Dalezios, N.; Ghane, M.; Qasemi, Z. Change detection of urban land use and urban expansion using GIS and RS, case study: Zanjan Province, Iran. *Int. J. Constr. Civ. Eng. IJCRCE* **2018**, *4*, 23–38.
15. Al-Bilbisi, H.H. Land use/cover change detection in arid and semi-arid areas of Northeastern Jordan using Landsat images. *Jordan J. Soc. Sci.* **2017**, *10*, 265–275.
16. Soffianian, A.; Ahmadiadoushan, M.; Yaghmael, L.; Falahatkar, S. Mapping and analyzing urban expansion using remotely sensed imagery in Isfahan, Iran. *World Appl. Sci. J.* **2010**, *9*, 1370–1378.
17. Al-Bilbisi, H.; Tateishi, R. Using satellite remote sensing data to detect land use/cover changes and to monitor land degradation in central Jordan. *J. Jpn. Soc. Photogramm. Remote Sens.* **2003**, *42*, 4–18. [[CrossRef](#)]
18. Weng, Q. Land use change analysis in Zhujiang Delta of China using satellite remote sensing, GIS and stochastic modeling. *J. Environ. Manag.* **2002**, *64*, 273–284. [[CrossRef](#)]
19. Al-Bilbisi, H. A two decades land use/cover change detection and land degradation monitoring in central Jordan using satellite images. *Jordan J. Soc. Sci.* **2012**, *5*, 133–149.
20. Department of Statistics (DOS) of Jordan. *Jordan in Figures Book*; Department of Statistics of Jordan: Amman, Jordan, 2018.
21. Bender, F. *Geology of Jordan*; Gebrüder Borntraeger: Berlin, Germany, 1974.
22. Potter, R.B.; Darmame, K.; Barham, N.; Nortcliff, S. Ever-growing Amman, Jordan: Urban expansion, social polarisation and contemporary urban planning issues. *Habitat Int.* **2008**, *33*, 81–92. [[CrossRef](#)]
23. Ministry of Municipal and Environment of Jordan. *National strategy for Jordan*; Ministry of Municipal and Environment of Jordan: Amman, Jordan, 1991.
24. Al-Bakri, J.; Duggah, M.; Brewer, T. Application of remote sensing and GIS for modeling and assessment of land use/cover change in Amman/Jordan. *J. Geogr. Inf. Syst.* **2013**, *5*, 509–519.
25. Jordan Meteorological Department (JMD). *Climatic Data Report*; Jordan Meteorological Department: Amman, Jordan, 2017.
26. Jensen, J.R. *Introductory Digital Image Processing: A Remote Sensing Perspective*, 3rd ed.; Prentice Hall: Upper Saddle River, NJ, USA, 2005.
27. Schowengerdt, R.A. *Remote Sensing: Models and Methods for Image Processing*, 3rd ed.; Academic Press: London, UK, 2006.
28. Sato, H.; Tateishi, R. Proposal for global land cover guideline legend based on FAO's LCCS. *Asian J. Geoinf.* **2002**, *3*, 35–46.
29. Campbell, J.B. *Introduction to Remote Sensing*; Guilford Press: New York, NY, USA, 2006.
30. Lillesand, T.M.; Kiefer, R.W. *Remote Sensing and Image Interpretation*, 3rd ed.; John Wiley & Sons, Inc.: New York, NY, USA, 2003.
31. Yang, X.; Lo, C.P. Using a time series of satellite imagery to detect land use and land cover changes in the Atlanta, Georgia metropolitan area. *Int. J. Remote Sens.* **2002**, *23*, 1775–1798. [[CrossRef](#)]

32. Singh, A. Digital change detection techniques using remotely-sensed data. *Int. J. Remote Sens.* **1989**, *10*, 989–1003. [[CrossRef](#)]
33. Xiao, J.Y.; Shen, Y.J.; Ge, J.F.; Tateishi, R.; Tang, C.Y.; Liang, Y.Q. Evaluating urban expansion and land use change in Shijiazhuang, China, by using GIS and remote sensing. *Landsc. Urban Plan. J.* **2006**, *75*, 69–80. [[CrossRef](#)]



© 2019 by the author. Licensee MDPI, Basel, Switzerland. This article is an open access article distributed under the terms and conditions of the Creative Commons Attribution (CC BY) license (<http://creativecommons.org/licenses/by/4.0/>).